Effects of resources and costs on diffusion dynamics

Yu-Shiuan Tsai

Department of Computer Science,
National Chiao Tung University,
1001 Ta Hsueh Road, Hsinchu 300,
Taiwan, Republic of China
E-mail: mathoowind@gmail.com

Chung-Yuan Huang*

Department of Computer Science and Information Engineering,
Research Center for Emerging Viral Infections,
Chang Gung University,
259 Wen Hwa 1st Road, Taoyuan 333,
Taiwan, Republic of China
Fax: +886-3-2118700
E-mail: gscott@mail.cgu.edu.tw
*Corresponding author

Abstract: Tipping point is one of the most important assessment indicators of epidemic outbreaks. Due to what we perceive as a too-strong emphasis on ways that the power-law connectivity distribution features of networks affect diffusion dynamics, two important factors have been overlooked: resources and costs. In this paper, we show that at odds with current thinking, a significant tipping point does exist when resources and costs are taken into consideration; and it is possible to control the spread of epidemics in scale-free networks as long as resources are restricted and the costs associated with an infection event are increased.

Keywords: tipping point; resources; transmission costs; scale-free networks; effective spreading rate.

Reference to this paper should be made as follows: Tsai, Y.S. and Huang, C.Y. (2010) 'Effects of resources and costs on diffusion dynamics', *Int. J. Intelligent Information and Database Systems*, Vol. 4, No. 1, pp.19–42.

Biographical notes: Yu-Shiuan Tsai received his BS (2002) and MS in Mathematics (2005) from National Taiwan University, Taiwan. He is pursuing his PhD in the department of Computer Science, National Chiao Tung University. His current research interests include complex networks and systems, social science models, and mathematical analysis.

Chung-Yuan Huang received his PhD in Computer Science (2005) from National Chiao Tung University, Taiwan. He is currently an Assistant Professor in the department of Computer Science and Information Engineering and a member of the Research Center for Emerging Viral Infections at Chang Gung University, Taiwan. His research interests include complex adaptive networks and systems, agent-based modelling and network-oriented simulation approaches for social science research, computational epidemiology, computational systems biology, and evolutionary computations.

1 Introduction

Interest in epidemiological issues associated with social networks has grown considerably ever since Watts and Strogatz (1998) first described their idea of small-world networks characterised by highly clustered connections and short paths between node pairs. Their work was followed by Barabási and Albert's (1999) description of scale-free networks that follow power-law connectivity distribution laws. Researchers are now regularly applying network-oriented approaches to analyse contagious disease diffusion processes (see, for example, Barabási and Albert's (1999), Dezsö and Barabási (2002), Huang et al. (2004, 2005a, 2005b), Moreno et al. (2003), Newman (2003), Newman and Watts (1999), Pastor-Satorras and Vespignani (2001a, 2001b, 2002a, 2002b, 2003), Watts (2003) and Watts and Strogatz (1998)). They note that the topological features of social networks exert considerable influence on diffusion dynamics and spreading situations associated with epidemics, which allow for subtle analyses that non-network-oriented approaches (e.g., system dynamics) are incapable of producing.

Whether or not tipping points exist when epidemics are spread through social networks is a major epidemiological issue currently being addressed by researchers from a range of disciplines (Boguñá and Pastor-Satorras, 2002; May and Lloyd, 2001; Pastor-Satorras and Vespignani, 2001a, 2001b, 2002a, 2002b, 2003). According to Pastor-Satorras and Vespignani, epidemics spread in scale-free networks do not have positive tipping points. Other researchers of diffusion dynamics and tipping points in scale-free networks have consistently concluded that regardless of transmission capability, all contagious diseases have high probabilities of stable spreading and survival in scale-free networks (Dezsö and Barabási, 2002; Liu et al., 2004; Volchenkov et al., 2002; Watts, 2003; Xu et al., 2007). For example, scale-free networks such as those associated with human sexual contact are currently being studied as capable (in terms of diffusion) yet vulnerable (in terms of prevention) platforms for the spread of diseases such as HIV/AIDS (Briesemeister et al., 2003; Gallos et al., 2005).

However, while new contagious diseases constantly emerge in different parts of the world, very few reach epidemic proportions or even survive in social networks; the majority dies almost immediately, which contradicts previous findings. This observation serves as motivation to take a more detailed look at limitations in transmission and interaction processes among individuals rather than the power-law connectivity distribution features of social networks – the focus of many epidemiological studies published in the past decade (Barabási, 2002; Buchanan, 2002; Watts, 2003). Two important factors associated with face-to-face interactions and daily contacts have been understudied: *resource limitations* and *transmission costs*. We acknowledge the importance of Pastor-Satorras and Vespignani's work on scale-free networks (in which node degrees satisfy power-law distributions), since their ideas have inspired numerous studies on tipping points and immunisation strategies. However, a closer inspection of their mathematical analyses and numerical simulations reveal what we believe are incorrect assumptions that daily interaction processes are *cost-free* and that the impacts of resource limitations and transmission costs are minimal. Such assumptions are beneficial in terms of mathematical equations and hypotheses and, therefore, suitable for studying internet viruses spread via e-mails with large numbers of recipient addresses. However, they are unrealistic and inaccurate when applied to biologically contagious diseases spread via face-to-face interactions and daily contacts.

Resources consumed by individuals during the process of spreading a contagious disease have five properties:

- they can be visible (e.g., seminal fluid, physical power) or invisible (e.g., time, energy)
- they are finite (e.g., time and energy spent on social interactions per day, which also follow normal distributions) and can be temporarily exhausted (e.g., elapsed time during interactions with other individuals and daily sexual contacts are limited in terms of consumptive energy)
- consumption of one kind of resource may entail consumption of other kinds, thereby reducing the total amount available (e.g., time and energy spent by HIV-positive individuals during sexual contacts)
- individual resources can recover or regenerate after a period of time (e.g., energy levels are revived by sleep)
- resources decrease during the course of a time unit (e.g., one day).

Furthermore, contagious carriers who expend resources on certain recipients cannot reuse the same resources on others; conversely, recipients cannot reuse resources spent on individual carriers.

For this project we simultaneously applied dynamic mean-field theory and a network-oriented approach to analyse the influences of resources and costs on diffusion dynamics and tipping points in scale-free networks. Our model analysis and simulation results indicate that

- when those resources and costs are taken into account, the diffusion dynamics of scale-free networks are very similar to those of homogeneous networks, including the presence of significant tipping points
- when transmission costs increase or individual usable resources decrease, tipping points in scale-free networks grow linearly and epidemic density curves shrink
- regardless of whether resources obey delta, uniform, or normal distributions, they have the same diffusion dynamics and tipping points as long as the average value of individual usable resources remains the same across different scale-free networks.

These conclusions can assist epidemiologists and public health professionals in their efforts to understand diffusion dynamics and tipping points and to revise current public health policies and immunisation strategies.

2 Diffusion dynamics in complex networks

In standard epidemiological models, individuals in any population can be classified into a limited number of states, including *Susceptible* (vulnerable to infection but not yet infected), *Infected* (capable of infecting others), and *Removed* (recovered, dead, or otherwise not posing any threat). Epidemiologists use combinations of these states to represent orders of transition between different epidemiological phases, giving their models names such as ‘SIR’ and ‘SIS’. Past epidemiological research has focused on the diffusion dynamics and spreading situations of biologically contagious diseases.

A growing number of researchers are currently studying non-biological and intangible concepts such as computer viruses, cultural influences, and rumours, ideas, and beliefs that exist in social networks and on the internet (Huang et al., 2005a; Lynch, 1998; Rogers, 2006). In Sections 2.1 and 2.2 we will review research on diffusion dynamics and tipping points in homogeneous networks (e.g., Erdös and Renyi's (1959) random and Watts and Strogatz's (1998) small-world) and non-homogeneous networks (e.g., Barabási and Albert's (1999) scale-free). Three types of complex networks that are currently being applied to epidemic simulations will be introduced in Section 2.3.

2.1 Diffusion dynamics and tipping points in homogeneous networks

In complex networks, nodes are used to represent entities in biological environments or on the internet (e.g., organisms and computers). Links indicate close relationships or specific interaction channels between two entities; those with direct connections are labelled *neighbours* (Newman, 2003; Watts, 2003). When simulating diffusion dynamics in complex networks, epidemiologists usually assume that nodes in complex networks run stochastically through a *Susceptible* $\rightarrow$ *Infected* $\rightarrow$ *Susceptible* cycle. During each time step, all susceptible nodes connected to one or more infected nodes are subject to a ν probability contagion rate. An effective spreading rate λ is defined as $\lambda = \nu/\delta$. *Infected* nodes recover at a δ probability rate and once again become *Susceptible*. Recovery rate δ can be assigned a value of 1 because it only affects contagious disease propagation time scales (Pastor-Satorras and Vespignani, 2001a).

Pastor-Satorras and Vespignani (2001a) define $\rho(t)$ as the density of infected nodes at time step t. As time approaches infinity, ρ can be represented as a steady-state density of infected nodes. Based on these definitions, they applied mean-field theory to their SIS epidemiological model and used Anderson and May's (1992) *homogeneous mixing hypothesis* to obtain

- a steady-state density ρ of infected nodes during long time periods (equation (1))
- the tipping point λ_c (equation 2):

$$\rho = \begin{cases} 0 & \text{if } \lambda < \lambda_c, \\ \dfrac{\lambda - \lambda_c}{\lambda} & \text{if } \lambda \geq \lambda_c, \end{cases} \tag{1}$$

$$\lambda_c = \frac{1}{<k>} \tag{2}$$

where $\langle k \rangle = \sum_k k p_k$ is the average vertex degree of the network and p_k the fraction of nodes in the network with vertex degree k. According to equations (1) and (2), positive and non-zero tipping points exist in homogeneous networks based on the SIS epidemiological model. A contagion becomes an epidemic if the effective spreading rate exceeds the tipping point $(\lambda \geq \lambda_c)$, otherwise it dies out. As shown in Figure 1, the SIS epidemiological model separates an infected state from a healthy state at tipping point λ_c. In other words, the main purpose of an SIS epidemiological model in a homogeneous network is to determine the presence of a positive tipping point proportional to the inverse of the average number of neighbours for each node, below which epidemics die and endemic states are impossible.

Figure 1 Phase transition diagram for epidemic simulations in homogeneous networks.

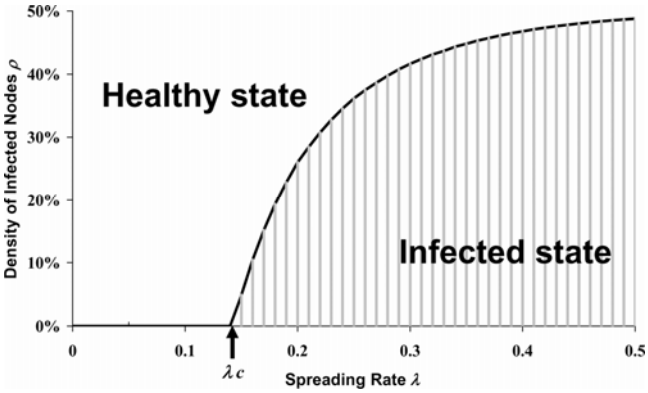

2.2 Diffusion dynamics and tipping points in scale-free networks

Pastor-Satorras and Vespignani (2003) argue that epidemics spread in scale-free social networks do not have positive tipping points. Asserting that the steady-state density ρ of infected nodes for the SIS epidemiological model in a Barabási and Albert (1999) scale-free network can be expressed as a function of the effective spreading rate λ, Pastor-Satorras and Vespignani compare it to a theoretical prediction for a homogeneous network. In this paper we refer to Barabási and Albert's network as a *BA scale-free network*, in which node degree follows a power-law distribution. As shown in Figure 2, the steady-state density ρ of infected nodes in a BA scale-free network reaches 0 in a continuous and smooth manner when the effective spreading rate λ decreases; this indicates the absence of any tipping point ($\lambda_c = 0$) in a BA scale-free network. As long as $\lambda > 0$, epidemics can stably spread throughout such a network and eventually reach a steady state. This explains why scale-free networks are fragile in epidemiological spreading situations. The internet, social networks, and human sexual contact webs all appear to be scale-free, meaning that computer viruses, innovative concepts, and sexually transmitted diseases can be stably spread even when initial contagion cases emerge in small and limited areas.

Figure 2 Steady-state density ρ of infected nodes as a function of effective spreading rate λ

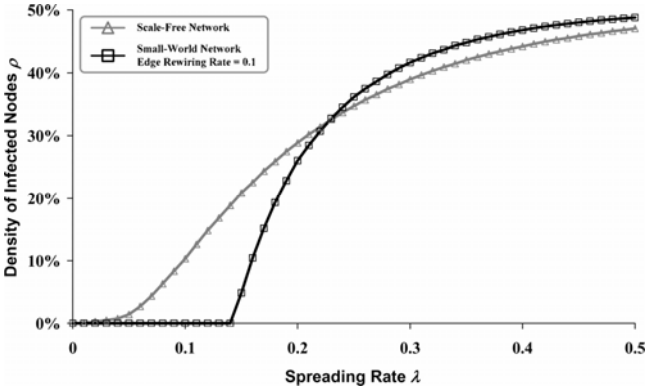

For finite size scale-free networks, Pastor-Satorras and Vespignani (2002b) introduce the node quantity-dependent concept of maximum connectivity k_c, which has the effect of restoring a connectivity fluctuation boundary and inducing an effective non-zero tipping point. According to the definition of maximum connectivity, $\langle k^2 \rangle$ in equation (3) has a clear finite value in a finite size scale-free network, but the tipping point vanishes as network size increases.

$$\lambda_c = \frac{<k>}{<k^2>}. \tag{3}$$

These conclusions explain the epidemic outbreak mechanisms of some biologically contagious diseases and computer viruses. According to traditional epidemiological theory, large-scale pandemics only occur when the effective spreading rate exceeds a specific tipping point. However, Pastor-Satorras and Vespignani claim that contagious diseases can proliferate in scale-free networks regardless of their effective spreading rate, an idea viewed as a major threat to public health and computer data.

2.3 Three types of complex networks applied to epidemic simulations

Complex networks are commonly used to represent structures for groups of individuals who exhibit interaction or relationship patterns (Barabási and Albert, 1999; Erdös and Renyi, 1959; Newman, 2003; Watts, 2003; Watts and Strogatz, 1998). Communities, cities, and countries – even our planet – can be defined as individual complex networks consisting of large-scale nodes and links. Each node represents one individual with status-determining attributes (often referred to as node-related information) such as epidemiological progress, contagiousness, or immunisation (Huang et al., 2005a; Xu et al., 2007). Connections between individuals are referred to as links, with different links representing different interpersonal relationships (Pastor-Satorras and Vespignani, 2002a, 2002b). In AIDS simulations they represent sexual relationships, in SARS simulations, close physical proximity (Huang et al., 2004, 2005b).

As shown in Figure 3 and Table 1, complex networks include Watts and Strogatz's (1998) small-world network, Barabási and Albert's (1999) scale-free network, and Erdös and Renyi's (1959) random network. They are popular among researchers who construct computational simulations of virtual societies, contagious diseases, internet viruses, and the spread of cultural beliefs and influences – all of which are affected by transmission routes.

Figure 3 Three complex network types

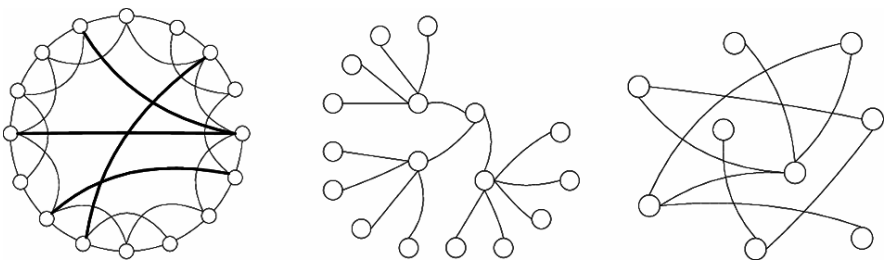

Table 1 Two complex networks categories

Category	*Specific network example*	*Clustering coefficient*	*Degree of separation*	*Connectivity distribution*
Homogeneous	Watts and Strogatz's (Watts and Strogatz, 1998) small-world network	High	Low	Normal
	Erdös and Renyi's (Erdös and Renyi, 1959) random network	Low	Low	Normal
Heterogeneous	Barabási and Albert's (Barabási and Albert, 1999) scale-free network	Low	Low	Power-law

Generating a Watts and Strogatz small-world network begins with a d-dimension ordered network with periodic boundary conditions, in which each node is connected to its z nearest neighbours, usually $z \geq 2d$ (Figure 4(a)) (Newman, 2003; Watts, 2003; Watts and Strogatz, 1998). Each link is randomly rewired to a new node with probability p (Figure 4(b)). Under adverse circumstances, this construction method can break the original ordered network into several isolated sub-graphs (Figure 4(d)). Newman and Watts (1999) simplified the Watts and Strogatz small-world network by replacing random link rewiring with random link additions (Figure 4(c)). The two networks are equivalent in cases where the probability p of edge rewiring or additions is small and the network scale is sufficiently large. Newman and Watts' small-world network thus avoids the problem of network breakage while preserving the positive characteristic of connecting each node in an d-dimensional ordered network with $2d$ neighbouring nodes. The original and new network versions retain the high local clustering properties of regular networks and dramatically reduce average path length by adding a small amount of randomness (Newman, 2003).

Figure 4 (a) One-dimensional ordered network with each node connected to four adjacent nodes; (b) Watts and Strogatz's (1998) small-world network with four rewired shortcuts; (c) Newman and Watts' (1999) improved small-world network with five additional shortcuts and (d) example of a broken Watts and Strogatz small-world network

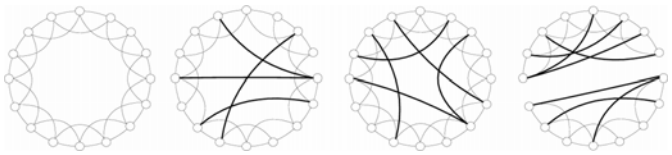

(a) (b) (c) (d)

Generating a BA scale-free network begins with a small number of nodes designated as z_0 (Barabási and Albert, 1999; Newman, 2003). During each iteration, a new node is introduced and connected to $z \leq z_0$ pre-existing nodes according to a probability based on each node's vertex degree. New nodes are preferentially attached to existing nodes that have large numbers of connections. This type of network exhibits short path lengths (i.e., low degree of separation) and power-law connectivity distribution properties, implying the existence of a small number of nodes with very large vertex degrees – similar to world wide web hyperlinks and human sexual contact webs.

Erdös and Renyi's (1959) random networks are generated by adding links between pairs of randomly chosen nodes with certain probabilities (see also Newman (2003)). They are capable of exhibiting a low degree of separation if sufficient numbers of links are added, but with little or no local clustering – an unusual situation in the real world.

3 Epidemic simulation model

In this section we will describe our use of a network-oriented simulation model, to indicate the presence of significant and positive tipping points when epidemics are spread in scale-free networks under realistic assumptions of resource limitations and transmission costs. The SIS epidemiological state transfer concept illustrated in Figure 5 was applied as the model's core architecture to simulate behavioural and transformative results emerging from individual interactions. A flowchart illustrating our proposed model is shown in Figure 6, and experimental parameters are described in Tables 2–5.

Figure 5 SIS epidemiological state transfer diagram

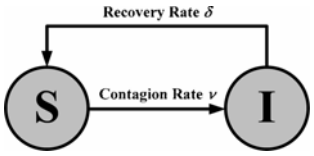

Figure 6 Simulation flowchart for a SIS epidemiological model

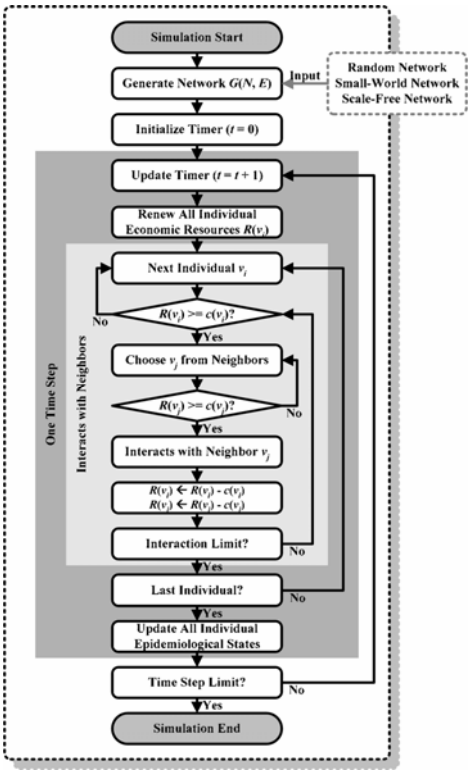

For our simulations we constructed a complex network $G(N, E)$ with $n = |N|$ nodes and $m = |E|$ links. In a complex network, N represents the node set, E the link set, $n = |N|$ the number of nodes (network order), and $m = |E|$ the number of links (network size) (Table 3). After building complex network G, all nodes not given *Infected* status (*InitialStatus_I* in Table 4) at the beginning of a simulation run were designated as *Susceptible*. To obtain a robust estimate, all diffusion dynamics and tipping points discussed in this paper were calculated as average values over 30 simulation runs.

Table 2 SIS epidemiological attributes

Attribute	*Type*	*Description*
ν	Real	Contagion rate. (also called 'infection rate' in SIS epidemiological model). Default range from 0.01 to 0.5 in 0.01 steps when $\delta = 1$
δ	Real	Reset rate (also called 'recovery rate' in SIS epidemiological model). Default value = 1.0
λ	Real	Effective spreading rate $\lambda = \nu / \delta$

Table 3 Network attributes

Attribute	*Type*	*Description*
Network type	Symbol	According to Network Type, a complex network for the SIS epidemic model can be built in the same manner as Watts and Strogatz's (1998) small-world homogeneous network and Barabási and Albert's (1999) scale-free network. If *Network type* = SWN, a small-world network is built; if *Network type* = SFN, a scale-free network is built. Default value = SFN
N	Set	Node set of a complex network
E	Set	Link set of a complex network
n	Integer	$n = \|N\|$ and represents total number of nodes in a complex networks built for a SIS epidemiological model, also called 'network order'
m	Integer	$m = \|E\|$ and represents total number of links in a complex network built for a SIS epidemiological model, also called 'network size'
Rewriting rate	Real	Specific parameter for Watts and Strogatz's small-world network. Generating a WS-SWN begins with 1-dimensional regular network with periodic boundary conditions. Each link is randomly rewired to a new node with a Rewiring Rate probability. Default value = 0.01

Table 4 Experiment setting attributes

Attribute	*Type*	*Description*
Time step limit	Integer	Total number of time steps during each simulation. Default value = 300
InitialStatus_I	Integer	Initial number of infected nodes at the beginning of epidemic simulation. Default value = 10

Table 5 Node-related attributes

Attribute	*Type*	*Description*
Cost	Integer	Transmission costs per interaction event. Default value = 1
R	Integer	Daily individual economic resources. Default value = 16
NowState	Symbol	Current epidemiological state
NextState	Symbol	Epidemiological state during next time step

Also, at the beginning of each time step, usable resources for each node v_i were reset to $R(v_i)$, meaning that all individuals either renewed and/or received supplemental resources (e.g., for most individuals, energy levels are revived after a night of sleep). In our later experiments, the statistical distribution of individual resources could be delta (fixed value r_{Constant}), uniform, normal, or power-law, as long as the average value $\langle r \rangle$ of individual resources satisfied equation (4):

$$\langle r \rangle = \frac{\sum_{i=1}^{|N|} R(v_i)}{|N|} = r_{\text{Constant}}. \tag{4}$$

Nodes randomly interacted with several neighbours during each time step, and consumed resources and costs during each interaction. From all of its $Neighbors(v_i)$, each node v_i randomly selected and interacted with one neighbouring node v_j. Following each interaction and regardless of the result, nodes v_i and v_j had transmission costs $c(v_i)$; $c(v_j)$ $0 \le c(v_i) \le R(v_i)$, and $0 \le c(v_j) \le R(v_j)$ deducted from their resources. If $R(v_i) < c(v_i)$ after an interaction, node v_i could not interact with other neighbours because all of its resources were expended. Otherwise, the interaction process was repeated, with nodes randomly selecting other neighbouring nodes until their resources were exhausted.

At each time step, the epidemiological state of each node was determined by a combination of behavioural rules, original epidemiological status, neighbours' epidemiological status, contagion rate ν, and recovery rate δ. Assume that an infected and contagious node v_a is adjacent to a susceptible and contagion-prone node v_b. When the two nodes come into contact, contagion rate ν determines whether or not v_b is infected by v_a. At the same time, an infected node v_a can recover at a recovery rate δ and once again become susceptible. The effective spreading rate λ is defined as ν/δ. Generally, recovery rate $\delta = 1$ and effective spreading rate $\lambda = \nu$. We define $\rho(t)$ as the density of infected nodes present at time step t. When time step t becomes infinitely large, ρ can be presented as a steady density of infected nodes.

4 Epidemic model analysis

Our mathematical model is based on the epidemic simulation model proposed by Pastor-Satorras and Vespignani (2001a), which neglects individual access to energy, time, and other finite resources. To incorporate these costs, we propose

$$\frac{\partial \rho_k(t,\lambda)}{\partial t} = -\rho_k(t,\lambda) + \lambda S_k[1-\rho_k(t,\lambda)]\,\theta(t,\lambda), \text{ where } S_k = \min\left(\frac{R}{c}, k\right). \tag{5}$$

The term $\rho_k(t) \ll 1$ is the probability that a node with k links is infected at time $t \geq 0$, where λ is the probability that in a time step equal to 1, a healthy node connected to one or more infected nodes will also become infected. The term $\theta(t, \lambda)$ is the average probability that a link will establish a connection with an infected node. Accordingly,

$$\theta(t, \lambda) = \sum_k \frac{kP(k)\rho_k(t, \lambda)}{\sum_s sP(s)} = \frac{1}{\langle k \rangle} \sum_k kP(k)\rho_k(t, \lambda),$$

with $P(s)$ a probability density function of node degree. According to the term S_k in equation (5) (with R representing average resources and c transmission costs), the spread of an infection is proportional to the minimum value of each active node's available resources (R/c) and number of links. The term $\theta(\lambda)$ is defined as the steady state of average probability that a link will establish a connection with an infected node:

$$\theta(\lambda) \equiv \lim_{t \to \infty} \theta(t, \lambda) = \frac{1}{\langle k \rangle} \sum_k kP(k)\rho_k(\lambda) \text{ for } \lambda \in [0, 1]. \tag{6}$$

Accordingly, $\theta(0) = 0$ and $\theta(1) = 1$. Using the mean field method with the stationary condition $\partial \rho_k(t, \lambda) / \partial t = 0$, from equation (5) we obtain

$$\rho_k(\lambda) \equiv \lim_{t \to \infty} \rho_k(t, \lambda) = \lim_{t \to \infty} \frac{\lambda S_k \theta(t, \lambda)}{1 + \lambda S_k \theta(t, \lambda)} = \frac{\lambda S_k \theta(t, \lambda)}{1 + \lambda S_k \theta(t, \lambda)},$$

with $\rho_k(\lambda)$ defined as the steady state of $\rho_k(t, \lambda)$. Substituting the above relation into equation (6) results in

$$\theta(\lambda) = \frac{1}{\langle k \rangle} \sum_k kP(k) \frac{\lambda S_k \theta(\lambda)}{1 + \lambda S_k \theta(\lambda)}.$$

Defining the tipping point λ_c as

$$\lambda_c \equiv \max\{\lambda \in [0, 1) : \theta(\lambda) = 0\} \tag{7}$$

succeeds because $\theta(0) = 0$ and $\theta(1) = 1$. Defining the right hand derivative as

$$\theta^{(l)}(\lambda) \equiv \left. \frac{\mathrm{d}^l \theta(x)}{\mathrm{d}x^l} \right|_{x=\lambda^+} \equiv \lim_{x \to \lambda} \frac{\mathrm{d}^l \theta(x)}{\mathrm{d}x^l} \text{ where } 0 \leq \lambda < x < 1, \text{ and } l \in \mathbb{Z}^+,$$

then

$$\theta^{(1)}(\lambda) = \frac{1}{\langle k \rangle} \sum_k \frac{kP(k)S_k[\theta(\lambda) + \lambda\theta^{(1)}(\lambda)]}{1 + \lambda S_k \theta(\lambda)} - \frac{1}{\langle k \rangle} \sum_k \frac{kP(k)\lambda S_k[S_k\theta(\lambda) + \lambda S_k \theta^{(1)}(\lambda)]}{\left[1 + \lambda S_k \theta(\lambda)\right]^2}$$

$$= \frac{1}{\langle k \rangle} \sum_k \frac{kP(k)S_k[\lambda\theta^{(1)}(\lambda)]}{1 + \lambda S_k \theta(\lambda)} + u_1(\lambda).$$

where

$$u_1(\lambda) = \frac{1}{\langle k \rangle} \sum_k \frac{kP(k)S_k\theta(\lambda)}{1 + \lambda S_k \theta(\lambda)} - \frac{1}{\langle k \rangle} \sum_k \frac{kP(k)\lambda S_k[S_k\theta(\lambda) + \lambda S_k \theta^{(1)}(\lambda)]}{\left[1 + \lambda S_k \theta(\lambda)\right]^2}$$

is the additional term. Inductively,

$$\theta^{(l)}(\lambda) = \frac{1}{\langle k \rangle} \sum_k \frac{kP(k)S_k[\lambda\theta^{(l)}(\lambda)]}{1+\lambda S_k \theta(\lambda)} + u_l(\lambda) \tag{8}$$

where $u_l(\lambda)$ is the additional term.

Note that the boundary condition $\theta(0) = 0$ implies that $\theta^l(0) = 0$ for $l = 1, 2, 3, \ldots$. According to equation (7), some $\lambda_c \in [0, 1)$ exists such that $\theta(\lambda_c) = 0$. If

$$m \equiv \min\{l : \theta^{(l)}(\lambda_c) > 0\}$$

then m is finite, which contradicts equation (7) due to the presence of some $\lambda_c^* \in (\lambda_c, 1)$ that satisfies $\theta(\lambda_c^*) = 0$.

Accordingly, from equation (8) we get

$$\theta^{(m)}(\lambda_c) = \frac{1}{\langle k \rangle} \sum_k P(k)S_k \lambda_c \theta^{(m)}(\lambda_c), \tag{9}$$

since $\theta(\lambda_c) = \theta^{(l)}(\lambda_c) = 0$ for $l < m$. Given that $\theta^{(m)}(\lambda_c) > 0$, we can divide both sides of equation (9) by $\theta^{(m)}(\lambda_c)$ to get

$$\lambda_c = \frac{\langle k \rangle}{\sum_k kP(k)S_k}.$$

Since $S_k = \min(R/c, k)$, the denominator can be divided into two parts to obtain

$$\lambda_c = \frac{\langle k \rangle}{\sum_{k \le \frac{R}{c}} k^2 P(k) + \sum_{k > \frac{R}{c}} \frac{R}{c} kP(k)}. \tag{10}$$

According to the first term in the denominator in equation (10), the variable k is smaller than R/c; therefore, substituting R/c for k makes the first term larger. Similarly, according to the second term the summation is smaller than the entire scope of k; therefore, substituting k for the entire scope also makes the second term larger. Thus,

$$\lambda_c \ge \frac{\langle k \rangle}{\sum_{k \le \frac{R}{c}} \left(\frac{R}{c}\right)^2 P(k) + \sum_k \frac{R}{c} kP(k)}. \tag{11}$$

Following the same method, making another substitution on the left side of the denominator in equation (11) results in

$$\lambda_c \ge \frac{\langle k \rangle}{\sum_k \left(\frac{R}{c}\right)^2 P(k) + \sum_k \frac{R}{c} kP(k)}.$$

Since $\sum_k P(k) = 1$, we arrive at

$$\lambda_c \ge \frac{\langle k \rangle}{\left(\frac{R}{c}\right)^2 + \frac{R}{c}\langle k \rangle} = \frac{1}{\left(\left(\frac{R}{c}\right)^2 \Big/ \langle k \rangle\right) + \frac{R}{c}} \to \frac{c}{R} \text{ as } \langle k \rangle \to \infty.$$

In summary, the lower bound of λ_c becomes smaller whether transmission cost c decreases or the average resource R increases. Accordingly, an individual's available resources expand when c/R is small, thereby increasing that individual's ability to contact almost all other personal network nodes. In the end, this model becomes identical to Pastor Satorras and Vespignani's.

5 Experimental results

To determine the reliability and robustness of our experimental results, and to ensure that our conclusions can be applied to various scale-free networks whose connectivity distribution probabilities satisfy $P(k) = k^{-\alpha}$ where $2 < \alpha \leq 3$ (e.g., sexual relationship networks, interpersonal networks, daily-contact networks, the internet), we built eight scale-free networks (Table 6) and eight small-world homogeneous networks (Table 7), all with different numbers of nodes and links, for our epidemic simulation experiments. All sensitivity analysis experiments were simulated using these networks to determine consistency in our results; no weakening or side effects were observed when node and link numbers were changed. As shown in Table 6, with the exception of node and link numbers (resulting in differences in average degree of separation), all parameter settings for the eight scale-free networks were identical and constructed using the same algorithm described in Section 2.3. The eight scale-free networks can be classified into four categories based on the number of nodes (1000, 2000, 10,000 or 20,000) or two categories based on average vertex degree (four or eight outgoing links per node). We designated scale-free simulation network #3 as our default; unless otherwise indicated, it was used to generate all results reported and discussed in this paper. According to those results, our research conclusions are not limited to our proposed epidemiological models based on the eight scale-free networks.

Table 6 Eight scale-free networks constructed using different numbers of nodes and average vertex degrees

	Barabási and Albert' (1999) *scale-free networks*							
	SFN#1	*SFN#2*	*SFN#3**	*SFN#4*	*SFN#5*	*SFN#6*	*SFN#7*	*SFN#8*
Number of nodes	1000	1000	2000	2000	10,000	10,000	20,000	20,000
Number of edges	2000	4000	4000	8000	20,000	40,000	40,000	80,000
Average vertex degrees	4	8	4	8	4	8	4	8
Exponent of power-law distribution	≈2.4	≈2.4	≈2.4	≈2.4	≈2.4	≈2.4	≈2.4	≈2.4
Average clustering coefficient	≈0.02	≈0.03	≈0.01	≈0.02	≈0.00	≈0.00	≈0.00	≈0.00
Average degree of separation	≈4.2	≈3.2	≈4.4	≈3.4	≈5.1	≈3.9	≈5.3	≈4.1

*Default network.

We initially used the first simulation experiment to show that an epidemic spread in a scale-free network has a non-zero, positive, and significant tipping point if resources and transmission costs are taken into consideration – a universal and general conclusion that differs from those reported by previous researchers. To evaluate how node and link numbers in scale-free networks affect their tipping points, all experiments were simulated using scale-free (Table 6) and small-world (Table 7) networks with different numbers of nodes and links. Usable resource value per individual was reset to 16 units at the beginning of each discrete time step. Transmission costs for each interaction process were designated as one unit, accounting for 6.25% of the individual's total usable resources.

Table 7 Eight small-world homogeneous networks for simulation experiments built using different numbers of nodes and average vertex degrees for comparison with eight corresponding scale-free networks

	Watts and Strogatz' (1998) *small-world networks with rewiring rate* = 0.01							
	SWN#1	*SWN#2*	*SWN#3*	*SWN#4*	*SWN#5*	*SWN#6*	*SWN#7*	*SWN#8*
Number of nodes	1000	1000	2000	2000	10,000	10,000	20,000	20,000
Number of edges	2000	4000	4000	8000	20,000	40,000	40,000	80,000
Average vertex degrees	4	8	4	8	4	8	4	8
Average clustering coefficient	≈0.28	≈0.37	≈0.28	≈0.37	≈0.28	≈0.37	≈0.28	≈0.37
Average degree of separation	≈7.0	≈4.4	≈7.9	≈4.9	≈9.9	≈6.0	≈10.6	≈6.5

We compared the relationship between effective spreading rate and steady density for the epidemiological model using three types of complex networks: small-world, scale-free without transmission costs, and scale-free with limited individual resources and transmission costs. As shown in Figure 7, the eight simulation experiment suites generated consistent results that did not become contradictory following adjustments in node and link numbers. We therefore suggest that the results can be applied to various scale-free networks used to simulate contagion scenarios.

The curves marked with triangles in Figure 7 show that the steady density of the epidemiological model based on scale-free networks reached 0 in a continuous and smooth manner when the effective spreading rate was decreased, indicating the absence of a tipping point in scale-free networks without transmission costs. The curves marked with squares show that contagious diseases do have tipping points in small-world homogeneous networks. In addition to being very similar to the curves marked with squares for small-world homogeneous networks, the curves marked with circles also show that contagious diseases have significant tipping points in scale-free networks when individual resources and transmission costs are considered (approximately 0.14 in Figure 7(a), (c), (e) and (g) and 0.10 in Figure 7(b), (d), (f) and (h). One conclusion

drawn from the results of the first simulation experiment is that individual resources, transmission costs, and average vertex degree exert significant impacts on diffusion dynamics and tipping points in scale-free networks, while node and link numbers have little impact.

Figure 7 Relationship between effective spreading rate and steady density of the SIS epidemiological model for three complex network platforms: small-world, scale-free with transmission costs, and scale-free with limited individual resources and transmission costs. The eight simulation experiment suites can be classified based on the number of nodes (1000, 2000, 10,000, or 20,000) and average vertex degree (four or eight outgoing links per node): (a) nodes = 1000, average degree = 4; (b) nodes = 1000, average degree = 8; (c) nodes = 2000, average degree = 4; (d) nodes = 2000, average degree = 8; (e) nodes = 10,000, average degree = 4; (f) nodes = 10,000, average degree = 8; (g) nodes = 20,000, average degree = 4 and (h) nodes = 20,000, average degree = 8

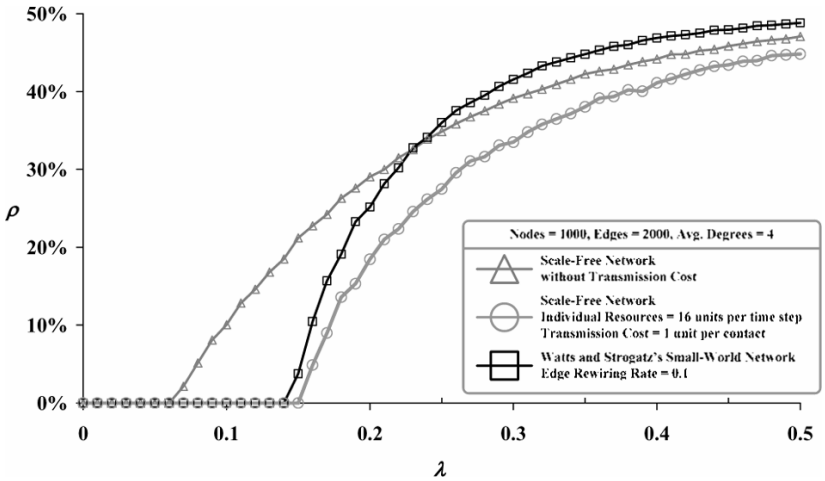

(a)

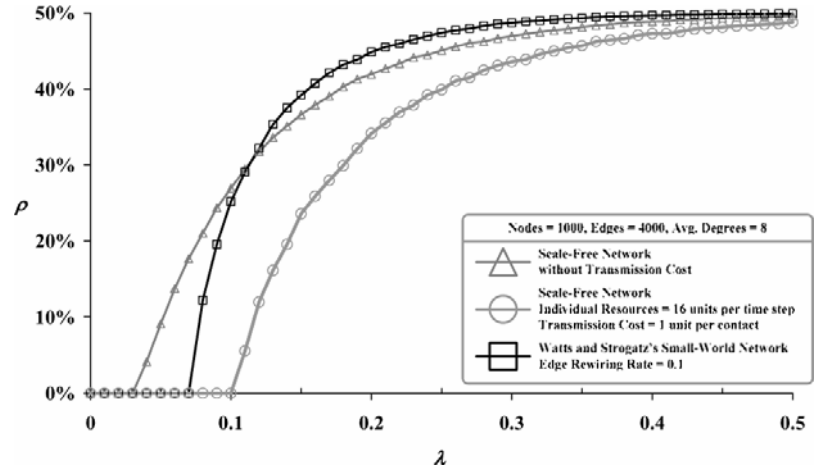

(b)

Figure 7 Relationship between effective spreading rate and steady density of the SIS epidemiological model on three types of complex network platforms: small-world, scale-free without transmission costs, and scale-free with limited individual resources and transmission costs (continued)

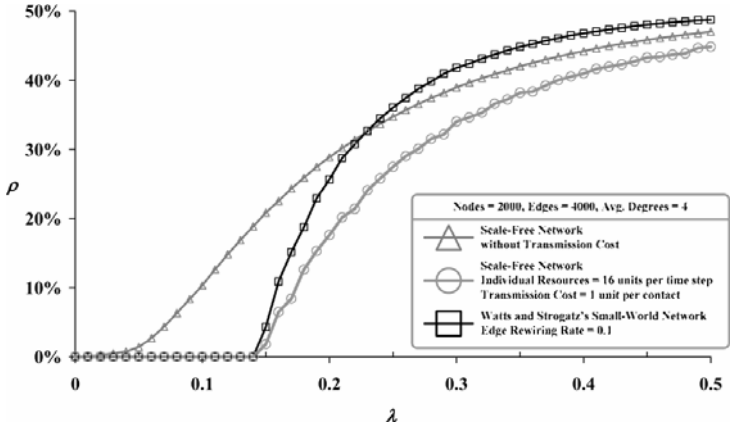

(c)

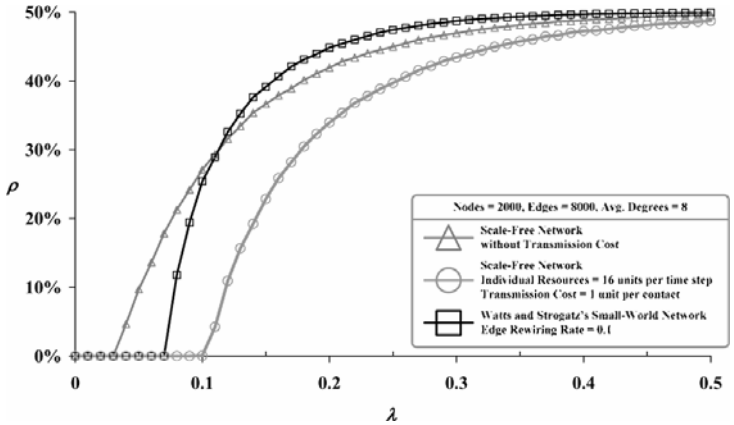

(d)

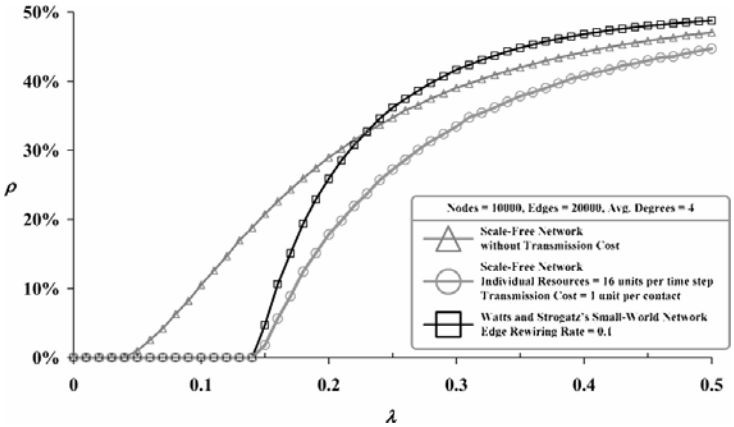

(e)

Figure 7 Relationship between effective spreading rate and steady density of the SIS epidemiological model on three types of complex network platforms: small-world, scale-free without transmission costs, and scale-free with limited individual resources and transmission costs (continued)

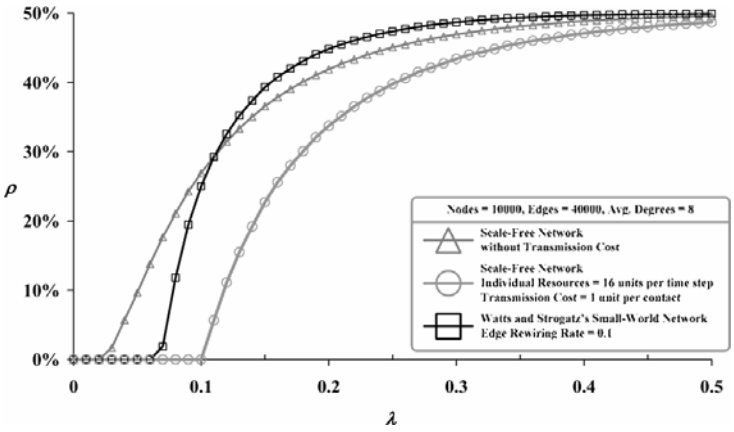

(f)

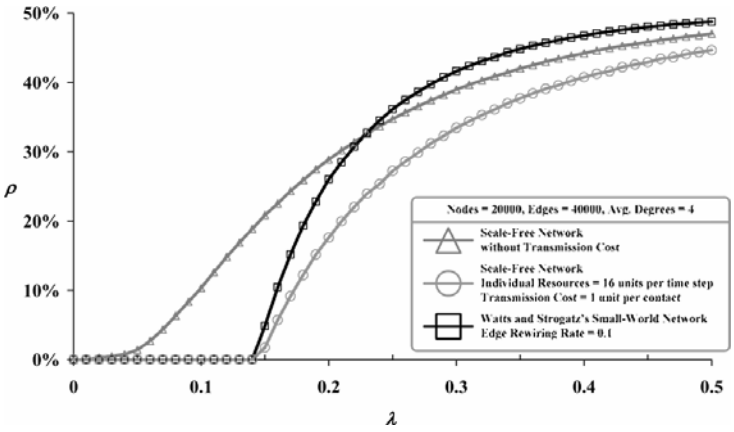

(g)

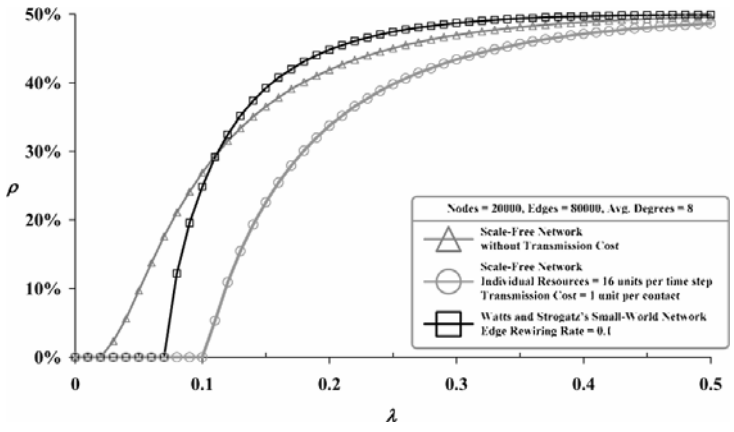

(h)

The second simulation experiment focused on relationships among tipping point, steady density curve, and the ratio of transmission costs to the total amount of an individual's usable resources (hereafter referred to as 'the ratio'). To evaluate the influence of the ratio on steady density curves and tipping points, we used ten usable resource values (4, 8, 12, 16, 20, 24, 28, 32, 36 and 40 units) and assigned the transmission cost for each interaction process as one unit accounting for 25%, 12.5%, 8.33%, 6.25%, 5%, 4.17%, 3.57%, 3.13%, 2.78% and 2.5% of the individual's total usable resources, respectively.

As shown in Figure 8(a), the tipping point significantly increased as the ratio grew. For instance, when the value of an individual's usable resources was set at eight units at the beginning of each discrete time step, the tipping point was approximately 0.22. This tipping point was significantly larger than that of a small-world network with the same number of nodes and links (Figure 7, curve marked with squares) and same average vertex degree (Figures 7(a), (c), (e) and (g)). The opposite was also true: when the value of an individual's usable resources was set at 40 units at the beginning of each discrete time step, the shape of the density curve was very close to that of the scale-free network without transmission costs (Figure 8(a), solid line); in addition, the tipping point was reduced to 0.09. As shown in Figure 8(b), a linear correlation was found between the tipping point and the ratio. We also observed that the density curve grew at a slower rate as the ratio increased (Figure 8(a)) – that is, the ratio and density had a negative linear correlation when the effective spreading rate exceeded the tipping point. One conclusion drawn from the results of our second simulation experiment is that when transmission costs increase or individual resources decrease, the tipping points of contagious diseases that are spread within scale-free networks grow linearly and density curves shrink linearly.

A comparison of the results from our mathematical model and the second simulation is shown in Figure 9. We used several degrees of probability for $P(k) = k^{-\alpha}$ and found that at an α of 2.7 or 2.65, the values for both curves exceeded that derived from the simulation experiment. The two curves matched at an α of 2.4.

Figure 8 Scale-free network #3: (a) the amount of an individual's resources affects density curves and tipping points and (b) linear relationship between the ratio of transmission costs to an individual's resources and tipping point

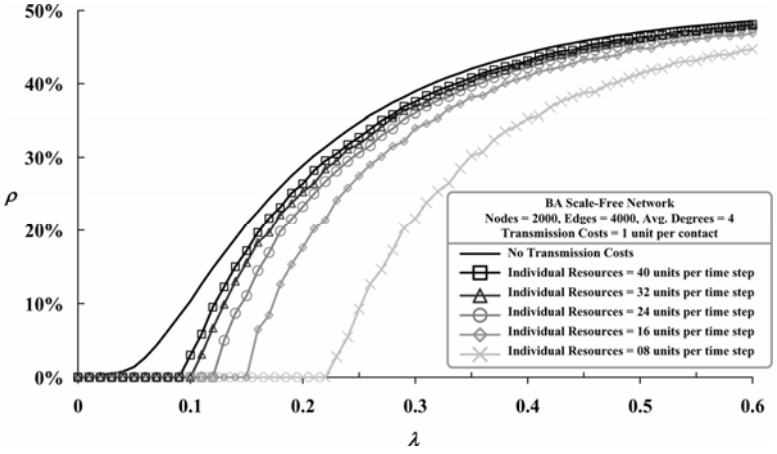

(a)

Figure 8 Scale-free network #3: (a) the amount of an individual's resources affects density curves and tipping points and (b) linear relationship between the ratio of transmission costs to an individual's resources and tipping point (continued)

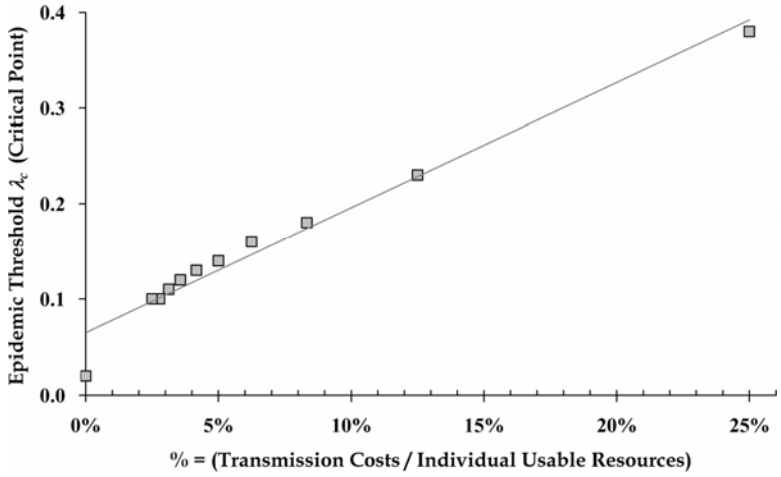

(b)

Figure 9 As a function of c/R ratio (transmission costs/individual resources) in BA scale-free networks, tipping point λ_c is used to analyse results from a simulation and three mathematical analyses

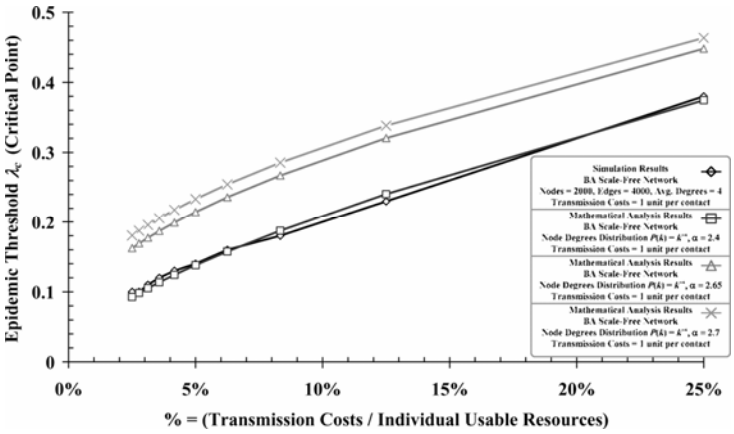

Our third simulation experiment was designed to investigate the effects of the statistical distribution of individual usable resources on the diffusion dynamics and tipping points of contagious diseases spread in scale-free networks. The specific goal was to determine how different statistical distribution types (delta, uniform, normal, power-law) of usable resources and their distribution parameters (average value and standard deviation in a normal distribution, or number of values and range in a uniform distribution) affect the steady density curves of contagious diseases spread in scale-free networks marked by limited individual resources and transmission costs (Figures 10(a)–(c) and 11(a)–(c)).

Figure 10 Scale-free network #3: (a) different statistical distribution types for individual resources affect the density curves and tipping points of contagious diseases spread within scale-free networks; (b) uniform ($n = 5$, $r = 2$) and normal (standard deviation = 2) distributions of individual resources with an average $\langle r \rangle$ value of 16 and (c) power-law distribution (degree = 3) of individual resources

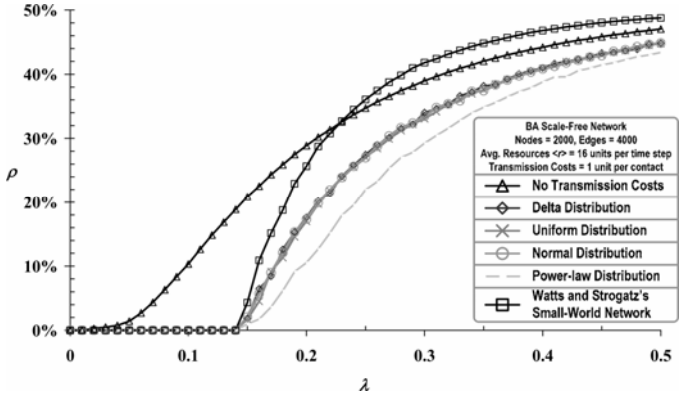

(a)

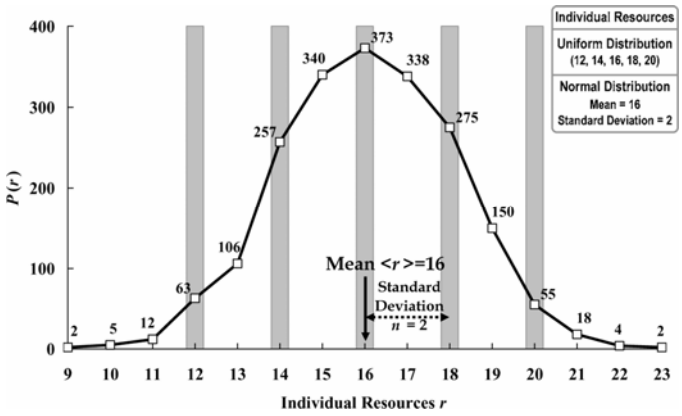

(b)

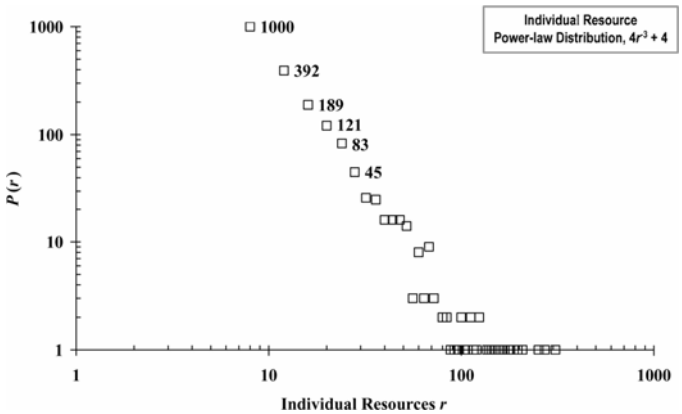

(c)

Figure 11 Scale-free network #3: (a) different statistical distribution types of individual resources affect the density curves and tipping points of contagious diseases spread within scale-free networks; (b) uniform (n = 5, r = 3) and normal (standard deviation = 3) distributions of individual resources with an average $\langle r \rangle$ value of 16 and (c) power-law distribution (degree = 3) of individual resources

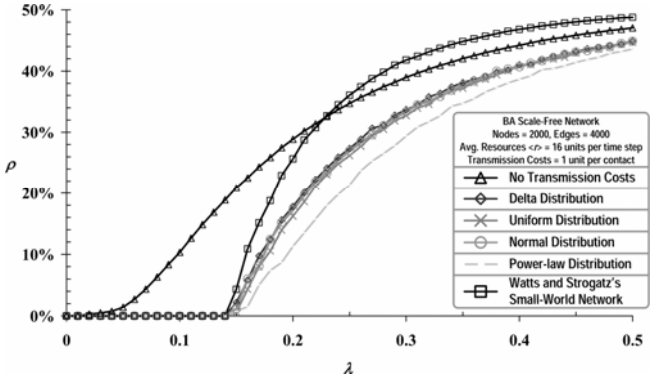

(a)

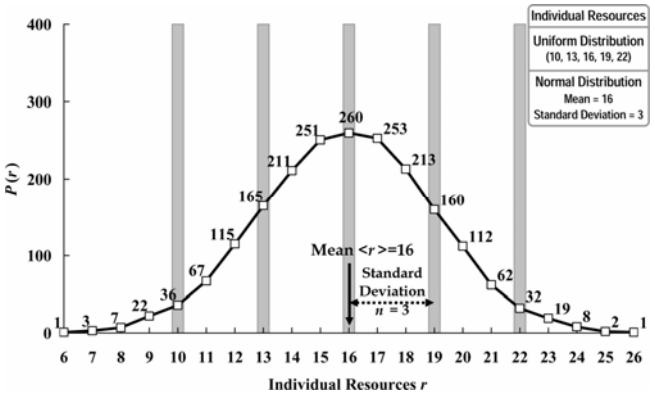

(b)

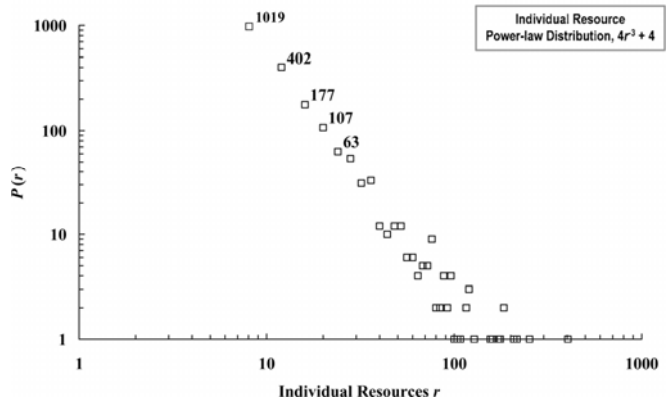

(c)

The density curves marked with diamonds, crosses, and circles in Figures 10(a) and 11(a) represent the delta (fixed value = 16), uniform, and normal distributions of resources, respectively; their distribution parameters are shown in Figures 10(b) and 11(b). The results show that the curves had the same tipping points (≈ 0.14) and that their density curves almost overlapped (indicating no statistically significant differences) when the average values of usable resources were equal. However, as shown in Figures 10(c) and 11(c), when those same resources reflected a power-law distribution (i.e., the majority of individuals had extremely limited resources while a small number had large amounts) and no correlation existed between the total amount of an individual's usable resources and vertex degree (number of neighbouring nodes), the resulting dashed density curve grew more slowly than those for the other three distributions, even when they all had the same tipping points.

As shown in Figures 10 and 11, the same results were produced as long as the average usable resource value was the same. The density curves and tipping points were almost the same across different distribution types, regardless of whether the resources obeyed a uniform distribution with a range of 2 or 3, or a normal distribution with a standard deviation of 2 or 3 (Figures 10(b) and 11(b)). According to the density curves shown in Figures 10(a) and 11(a), we suggest that to facilitate experiments without affecting simulation results, as long as researchers ensure that usable resources do not obey a power-law distribution, then at the beginning of each discrete time step they can simply assign usable resources for each individual as the fixed average value $\langle r \rangle$ of the statistical distribution derived from the real-world scenario.

6 Discussion and conclusion

We will use the 2002–2003 Severe Acute Respiratory Syndrome (SARS) outbreak as an example of a practical application of our results. The SARS coronavirus is propagated over short distances and can survive in air for several hours to several days. During the outbreak, the Singaporean government enacted a body temperature measurement policy, Hong Kong enforced policies such as hand washing and surgical mask usage, and the Taiwan government applied both. These, and other potential policies, can be divided into two types, with the first aimed at decreasing propagation. Examples include home quarantines for individuals suspected of having contact with infected individuals for a period equal to twice the known SARS latency period. As part of this policy, public health workers take the body temperatures of large numbers of individuals entering public spaces. Anyone with a fever exceeding 37ºC is detained and instructed to not come into contact with other individuals. The second type is aimed at increasing propagation costs for infected individuals. Examples include appeals to the general public to regularly wash hands, wear surgical masks, and maintain high levels of cleanliness. Vaccines and anti-virus medicines also belong to this category, as do requests for individuals to avoid public places as much as possible. It is generally believed that the speed with which both types of policies were put into place by the Hong Kong, Taiwan, and Singapore governments were positive factors in the successful control of the SARS epidemic.

In this study we investigated how resources and transmission costs influence diffusion dynamics and tipping points in scale-free networks. According to the results of our first experiment, when resources and transmission costs are taken into consideration,

tipping points exist when contagion events occur in scale-free networks. Our second experiment results provide insight into how the ratio of the cost of a single contagion event to the total amount of an individual's resources affects density curves and tipping points. When transmission costs increase, or when the total amount of an individual's resources decrease, the tipping point of a contagion event in a scale-free network grows and density is reduced at certain transmission rates. Results from our third experiment indicate that regardless of whether available resources obey a delta, uniform, or normal distribution, they have the same density curves and tipping points as long as the average resource value remains the same across different networks.

Acknowledgement

This work was supported in part by the Republic of China National Science Council (grant no. NSC 97-2221-E-182-046), Chang Gung University (no. UERPD270281), and Chang Gung Memorial Hospital (no. CMRPD260022).

References

Anderson, R.M. and May, R.M. (1992) *Infectious Diseases in Humans*, Oxford University Press, Oxford, UK.

Barabási, A.L. (2002) *Linked: The New Science of Networks*, Perseus Books Group, Cambridge, MA.

Barabási, A.L. and Albert, R. (1999) 'Emergence of scaling in random networks', *Science*, Vol. 286, No. 5439, pp.509–512.

Boguñá, M. and Pastor-Satorras, R. (2002) 'Epidemic spreading in correlated complex networks', *Physical Review E*, Vol. 66, p.047104.

Briesemeister, L., Lincoln, P. and Porras, P. (2003) 'Epidemic profiles and defense of scale-free networks', *Proceedings of ACM CCS Workshop on Rapid Malcode (WORM '03)*, Washington, DC, pp.67–75.

Buchanan, M. (2002) *Nexus: Small Worlds and the Groundbreaking Theory of Networks*, W.W. Norton & Company, New York.

Dezsö, Z. and Barabási, A.L. (2002) 'Halting viruses in scale-free networks', *Physical Review E*, Vol. 65, p.055103.

Erdös, P. and Renyi, A. (1959) 'On the evolution of random graphs', *Publication of the Mathematical Institute of the Hungarian Academy of Science*, Vol. 5, pp.17–60.

Gallos, L.K., Cohen, R., Argyrakis, P., Bunde, A. and Shlomo, H. (2005) 'Stability and topology of scale-free networks under attack and defense strategies', *Physical Review Letters*, Vol. 94, p.188701.

Huang, C.Y., Sun, C.T., Hsieh, J.L. and Lin, H. (2004) 'Simulating SARS: small-world epidemiological modeling and public health policy assessments', *Journal of Artificial Societies and Social Simulation*, Vol. 7, No. 4, pp.1–28, Available online at http://jasss.soc.surrey.ac.uk/7/4/2.html

Huang, C.Y., Sun, C.T. and Lin, H.C. (2005a) 'Influence of local information on social simulations in small-world network models', *Journal of Artificial Societies and Social Simulation*, Vol. 8, No. 4, pp.1–26, Available online at http://jasss.soc.surrey.ac.uk/8/4/8.html

Huang, C.Y., Sun, C.T., Hsieh, J.L., Chen, Y.M.A. and Lin. H. (2005b) 'A novel small-world model: using social mirror identities for epidemic simulations', *Simulation: Transactions of the Society for Modeling and Simulation International*, Vol. 81, No. 10, pp.671–699.

Liu, Z.H., Lai, Y.C. and Ye, N. (2004) 'Propagation and immunization of infection on general networks with both homogeneous and heterogeneous components', *Physical Review E*, Vol. 67, p.031911.

Lynch, A. (1998) *Thought Contagion: How Belief Spreads Through Society*, Basic Books, New York.

May, R.M. and Lloyd, A.L. (2001) 'Infection dynamics on scale-free networks', *Physical Review E*, Vol. 64, p.066112.

Moreno, Y., Gómez, J.B. and Pacheo, A.F. (2003) 'Epidemic incidence in correlated complex networks', *Physical Review E*, Vol. 68, p.035103.

Newman, M.E.J. (2003) 'The structure and function of complex networks', *SIAM Review*, Vol. 45, pp.167–256.

Newman, M.E.J. and Watts, D.J. (1999) 'Scaling and percolation in the small-world network model', *Physical Review E*, Vol. 60, pp.7332–7342.

Pastor-Satorras, R. and Vespignani, A. (2001a) 'Epidemic spreading in scale-free networks', *Physical Review Letters*, Vol. 86, No. 4, pp.3200–3203.

Pastor-Satorras, R. and Vespignani, A. (2001b) 'Epidemic dynamics and endemic states in complex networks', *Physical Review E*, Vol. 63, p.066117.

Pastor-Satorras, R. and Vespignani, A. (2002a) 'Immunization of complex networks', *Physical Review E*, Vol. 65, p.036134.

Pastor-Satorras, R. and Vespignani, A. (2002b) 'Epidemic dynamics in finite size scale-free networks', *Physical Review E*, Vol. 65, p.035108(R).

Pastor-Satorras, R. and Vespignani, A. (2003) 'Epidemics and immunization in scale-free networks', in Bornholdt, S. and Schuster, H.G. (Eds.): *Handbook of Graph and Networks*, Wiley-VCH, Berlin, pp.113–132.

Rogers, E.M. (2006) *Diffusion of Innovations*, 5th ed., The Free Press, New York.

Volchenkov, D., Volchenkov, L. and Blanchard, P. (2002) 'Epidemic spreading in a variety of scale-free networks', *Physical Review E*, Vol. 66, p.046137.

Watts, D.J. (2003) *Six Degrees: The Science of a Connected Age*, W.W. Norton & Company, New York.

Watts, D.J. and Strogatz, S.H. (1998) 'Collective dynamics of 'small-world' networks', *Nature*, Vol. 393, No. 6684, pp.440–442.

Xu, X.J., Zhang, X. and Mendes, J.F.F. (2007) 'Impacts of preference and geography on epidemic spreading', *Physical Review E*, Vol. 76, p.056109.

Note

1 Simulations available as Java applications at http://groups.google.com/group/canslab; for source code, please contact the authors.